Turbulent Measurements in a Small Subtropical Estuary with Semidiurnal Tides

Mark Trevethan[1]; Hubert Chanson[2]; and Richard Brown[3]

Abstract: Since predictions of scalar dispersion in small estuaries can rarely be predicted accurately, new field measurements were conducted continuously at relatively high frequency for up to 50 h (per investigation) in a small subtropical estuary with semidiurnal tides. The bulk flow parameters varied in time with periods comparable to tidal cycles and other large-scale processes. The turbulence properties depended upon the instantaneous local flow properties. They were little affected by the flow history, but their structure and temporal variability were influenced by a variety of parameters including the tidal conditions and bathymetry. A striking feature of the data sets was the large fluctuations in all turbulence characteristics during the tidal cycle, and basic differences between neap and spring tide turbulence.

DOI: 10.1061/(ASCE)0733-9429(2008)134:11(1665)

CE Database subject headings: Turbulence; Estuaries; Reynolds stress; Measurement; Tidal currents.

Introduction

In natural estuaries, turbulent mixing is critical to sediment transport, release of nutrient-rich wastewater into ecosystems and the water quality effects of storm-water runoff during flood events. Relatively little systematic research has been conducted on the turbulence characteristics in natural estuarine systems particulary in small systems. Past measurements were conducted typically for short periods, or in bursts, sometimes at low frequency (Shiono and West 1987; Kawanisi and Yokosi 1994; Ham et al. 2001; Voulgaris and Meyers 2004). Herein the turbulence characteristics of a small subtropical estuary with semidiurnal tides are examined with measurements being obtained continuously at relatively high frequency throughout a tidal cycle. The detailed results highlight the large fluctuations in all turbulence characteristics during the tidal cycle, and its temporal variability.

Turbulence Measurements in Small Subtropical Estuary

A series of detailed turbulence field measurements were conducted in a small estuary of Eastern Australia with a semidiurnal tidal regime (Table 1). The estuarine zone was 3.8 km long, about 1–2 m deep midstream (Fig. 1). With a narrow, elongated, and meandering channel (Chanson et al. 2005a), the estuary is a drowned river valley (coastal plain) type with a small, sporadic freshwater inflow, a cross section which deepens and widens towards the mouth, and surrounded by extensive mud flats. Fig. 1 includes some surveyed cross sections, in which the vertical elevations are related to the Australian height datum (AHD). The mean sea level is also shown. Although the tides are semidiurnal, the tidal cycles have slightly different periods and amplitudes indicating that a diurnal inequality exists. Table 1 summarizes the seven field studies conducted between 2003 and 2006 during which a range of field conditions were tested: tidal conditions from neap tides (Studies E6 and E7) to spring tides (Studies E3 and E5), and different bathymetry from midestuary (Studies E5 and E6) to the upper estuary (Study E7).

Turbulent velocities were measured with acoustic Doppler velocimetry (ADV) [i.e., a Sontek UW ADV (10 MHz) equipped with a 5 cm downlooking three-component sensor, and a Sontek micro-ADV (16 MHz) with a 5 cm side looking two-component head (Table 1, column 4)]. The velocity measurements were performed continuously at high frequency for 8–50 h during various tide conditions (Table 1, columns 5 and 6). A thorough postprocessing technique was developed and applied to remove electronic noise, physical disturbances, and Doppler effects (Chanson et al. 2005b). The field experience demonstrated that the gross ADV signals were unsuitable, and often led to inaccurate time-averaged flow properties. Herein only postprocessed data are discussed.

The postprocessed data sets included the three instantaneous velocity components V_x, V_y, and V_z where x is the longitudinal direction positive downstream; y is the transverse direction positive towards the left bank; and z is the vertical direction positive upwards. The turbulent velocity fluctuation was defined as $v = V - \bar{V}$ where V was the instantaneous (measured) velocity component and $\bar{V}$ was the variable-interval time average (VITA) velocity. A cutoff frequency was selected with an averaging time greater than the characteristic period of fluctuations, and smaller than the characteristic period for the time evolution of the mean properties. The selection of the cutoff frequency was derived from a sensitivity analysis. Herein all turbulence data were processed using samples that contain 5,000 data points (200 s) and calculated every 10 s along the entire data sets. The turbulence analysis

[1]Ph.D. Graduate, Division of Civil Engineering, The Univ. of Queensland, Brisbane QLD 4072, Australia.

[2]Professor, Division of Civil Engineering, The Univ. of Queensland, Brisbane QLD 4072, Australia (corresponding author). E-mail: h.chanson@uq.edu.au

[3]Senior Lecturer, School of Engineering Systems, Q.U.T., Brisbane QLD 4000, Australia.

Note. Discussion open until April 1, 2009. Separate discussions must be submitted for individual papers. The manuscript for this technical note was submitted for review and possible publication on December 28, 2006; approved on March 13, 2008. This technical note is part of the ***Journal of Hydraulic Engineering***, Vol. 134, No. 11, November 1, 2008. ©ASCE, ISSN 0733-9429/2008/11-1665–1670/$25.00.

Table 1. Turbulence Field Measurements at Eprapah Creek QLD, Australia

Ref.	Dates	Tidal range (m)	ADV system(s) (MHz)	Sampling rate (Hz)	Sampling duration	Sampling volume
E1	April 4, 2003	1.84	10	25	9×25 min	AMTD 2.1 km, 14.2 m from left bank, 0.5 m below surface.
E2	July 17, 2003	2.03	10	25	8 h	AMTD 2.0 km, 7.7 m from left bank, 0.5 m below surface.
E3	November 24, 2003	2.53	10	25	7 h	AMTD 2.1 km, 10.7 m from left bank, 0.5 m below surface.
E4	February 2, 2004	1.81	10	25	6 & 3 h	AMTD 2.1 km, 10.7 m from left bank, 0.052 m above bed.
E5	March 8–9, 2005	2.37	10	25	25 h	AMTD 2.1 km, 10.7 m from left bank, 0.095 m above bed.
E6	May 16–18, 2005	1.36	10 & 16	25	49 h	AMTD 2.1 km, 10.7 m from left bank, 0.2 & 0.4 m above bed.
E7	June 5–7, 2006	1.58	10 & 16	25 & 50	50 h	AMTD 3.1 km, 4.2 m from right bank, 0.2 & 0.4 m above bed.

Note: AMTD=adopted middle thread distance measured upstream from the river mouth.

yielded the first four statistical moments of each velocity component, the tensor of instantaneous Reynolds stresses, and the statistical moments of the tangential stresses. An autocorrelation analysis yielded the Eulerian dissipation and integral time scales, τ_E and T_E, respectively, for each velocity component. Herein τ_E was calculated using the method of Hallback et al. (1989) extended by Fransson et al. (2005). Turbulence statistics were not evaluated when more 20% of the 5,000 data points were corrupted/repaired during the ADV data postprocessing.

Turbulence Properties in Small Estuary

Bulk Flow Properties

The bulk parameters including the water depth and time-averaged longitudinal velocity were time dependant, varying with periods comparable to tidal cycles and other large-scale processes. This is illustrated in Figs. 2 and 3 showing the water depth, water conductivity, and time-averaged longitudinal velocities $\overline{V_x}$ recorded midestuary. Fig. 2 presents the water depth and conductivity data recorded midestuary during neap tide conditions. The results exhibit some tidal asymmetry during a 24 h 50 min period with a smaller (minor) tidal cycle followed by a larger (major) tidal amplitude. The water conductivity variations were driven primarily by the ebb and flood tides. The moderate range of specific conductivity seen in Fig. 2 was typical of neap tide conditions in the absence of freshwater runoff.

Fig. 3 presents $\overline{V_x}$ in the middle of the deepest channel during neap and spring tides. For all field studies at midestuary, the largest velocity magnitude occurred just before and after the low tide, with the flood velocities always larger than ebb velocities. Kawanisi and Yokosi (1994) observed similar maximum flood and ebb

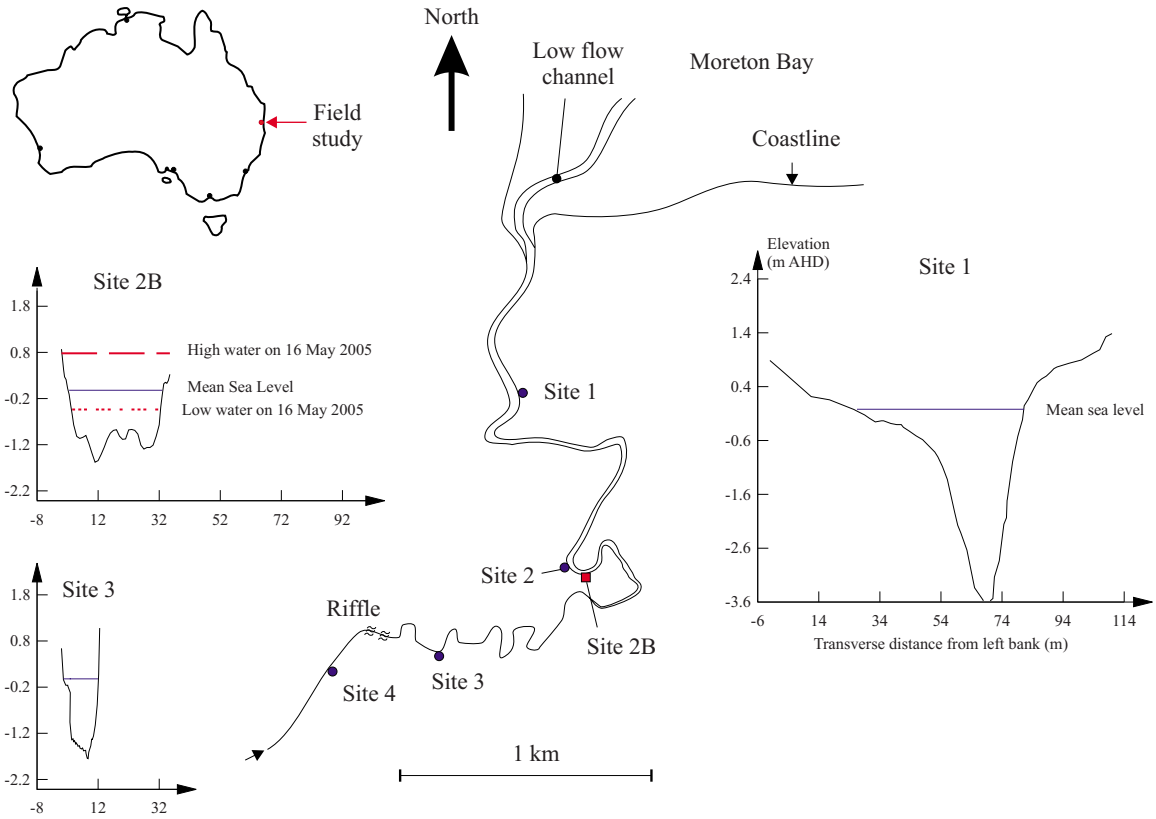

Fig. 1. Sketch of Eprapah Creek estuarine zone and surveyed cross sections

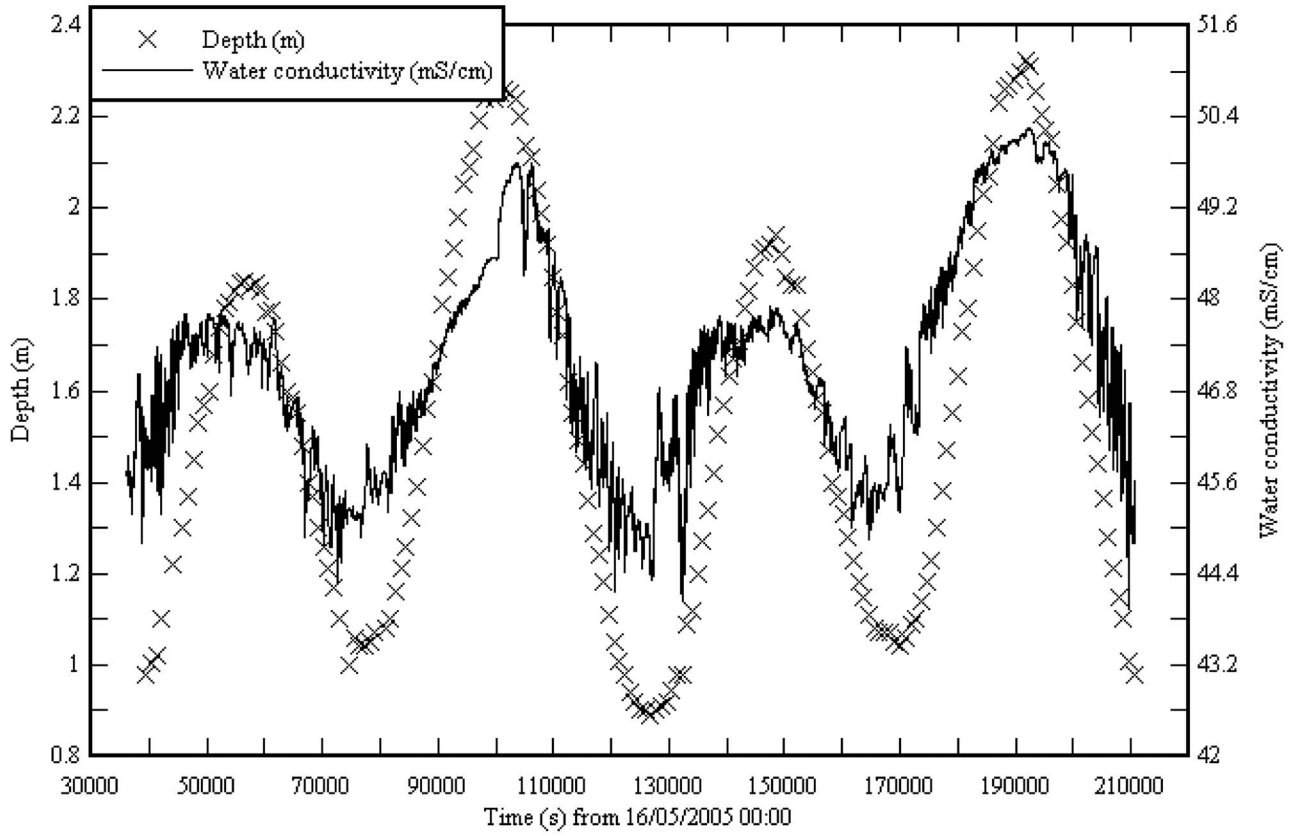

Fig. 2. Measured water depth and water conductivity during neap tide conditions (Field Work E6)

velocities around low tide and larger flood velocities, in an estuarine channel in Japan. Some multiple flow reversal events around high tides and some long-period velocity oscillations around midtide may be noted. Fig. 3(a) shows an example of long-period velocity oscillations during the flood tide between $t=105{,}000$ and 125,000 s where the time t is counted since midnight (00:00) on the first day of the study. Fig. 3(b) presents an illustration of multiple flow reversals about high tide between $t=50{,}000$ and 65,000 s. These low-frequency velocity oscillations were generated by some resonance caused by the tidal forcing interacting

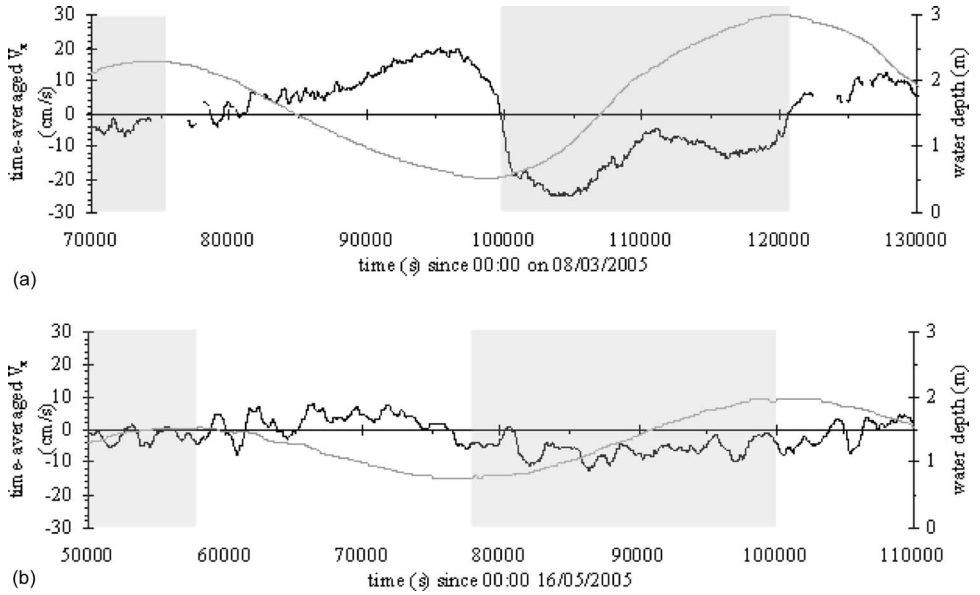

Fig. 3. Time-averaged longitudinal velocity $\overline{V_x}$ (positive downstream) and water depth as functions of time during full tidal cycle: (—) time-averaged longitudinal velocity (cm/s); (—) water depth at site 2B: (a) time-averaged longitudinal velocity data collected at 0.1 m above bed during spring tides (Study E5); (b) time-averaged longitudinal velocity data collected at 0.4 m above bed during neap tides (Study E6)

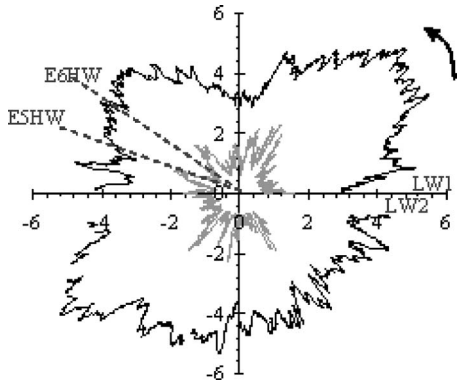

Fig. 4. Standard deviations of longitudinal velocity v_x' (cm/s) during major tidal cycle in spring and neap tide conditions: (●) Field Study E5 (spring tide) ADV with sensor at 0.1 m above bed; and (●) Field Study E6 (neap tide) with ADV sensor at 0.4 m above bed

with the estuary topography and the outer bay system (Trevethan et al. 2006). These effects were more noticeable during neap tide conditions and seemed more pronounced in the upper estuary.

Turbulence Properties

The field observations showed systematically large standard deviations of all velocity components at the beginning of the flood tide for all tidal cycles. Standard deviations of the longitudinal velocity v_x' are shown in Fig. 4 for two tidal cycles in spring and neap tides, presenting the magnitude of v_x' from a low water (LW1) to the next low water (LW2). The data are presented in a circular plot where the radial coordinate is the turbulent property (herein v_x'), and the angular coordinate is the time relative to the next low water. From the first low water, the time variation of the data progress anticlockwise until the next low water. The high and low waters are indicated.

The standard deviations of all velocity components were two to four times larger in spring tides than during neap tides (Fig. 4). v_x' was systematically larger during the flood tide than during the ebb tide, while there were significant fluctuations in velocity standard deviations during the entire tidal cycle. Kawanisi and Yokosi (1994) observed similar larger measured velocity standard deviations during flood tide in a tidal channel in Japan. The horizontal turbulence ratio v_y'/v_x' was approximately equal to 1 for spring and neap tide conditions and larger than laboratory observations in straight prismatic rectangular channels $v_y'/v_x'=0.5-0.7$ as reported in Nezu and Nakagawa (1993). The vertical turbulence ratio v_z'/v_x' was similar to the observations of Shiono and West (1987) and Kawanisi and Yokosi (1994) in estuaries, and of Nezu and Nakagawa (1993) and Xie (1998) in laboratory open channels. v_z'/v_x' was approximately half of the horizontal turbulence intensity v_y'/v_x', implying some turbulence anisotropy.

The skewness and excess kurtosis, which gave some information on the temporal distribution of the turbulent velocity fluctuation around its mean value, of all velocity components significantly varied with time during each tidal cycle. The normalized third (skewness) and fourth (excess kurtosis) moments of the velocity fluctuations appeared to be within the range $-0.6-+0.6$, and $-1-+2$, respectively, close to the observations of Shiono and West (1987) in an estuary where velocity skewness and excess kurtosis were observed within the ranges $-0.5-+0.5$, and $-4-+4$, respectively. They were also comparable with the laser Doppler velocimetry (LDV) data of Niederschultze (1989) and Tachie (2001) in developing turbulent boundary layers in laboratory channels.

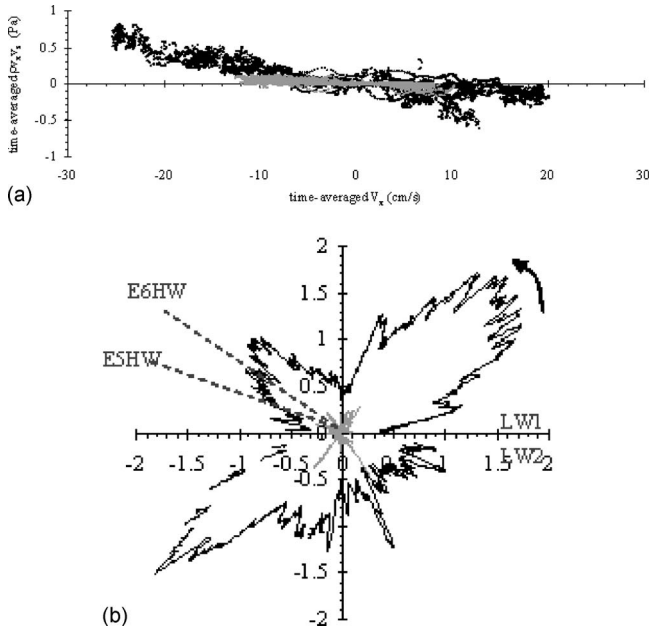

Fig. 5. Tangential Reynolds stress $\rho v_x v_z$ during spring and neap tide conditions (Field Works E5 and E6, respectively) (●) FIeld Work E5, (●) Field Work E6; (a) time-averaged Reynolds stress $\rho v_x v_z$ as function of time-averaged longitudinal velocity; (b) standard deviations of tangential Reynolds stress $(\rho v_x v_z)'$ (Pa) during major tidal cycle

The tangential Reynolds shear stresses varied with the tide during all field works. Fig. 5(a) illustrates the trend for two fields studies by showing the time-averaged Reynolds stress the $\rho v_x v_z$ as a function of $\overline{V_x}$. The turbulent stress $\rho v_x v_z$ was predominantly positive during the flood tide and negative during the ebb tide [Fig. 5(a)]. The present trend was consistent with the data of Osonphasop (1983), Kawanisi and Yokosi (1994), and Ham et al. (2001) in tidal channels. The negative correlation between $\rho v_x v_z$ and $\overline{V_x}$ was also consistent with traditional boundary layer results (Xie 1998; Tachie 2001). The magnitudes of the time-averaged tangential Reynolds stresses were at least an order of magnitude larger during spring tides than those for neap tide conditions. The larger magnitude of Reynolds shear stresses derived from the increased tidal forcing.

The standard deviations of the tangential Reynolds stresses increased with increasing $\overline{V_x}$. The magnitude of the standard deviations of all tangential Reynolds stresses were one order of magnitude greater in spring tides than those observed at neap tides [Fig. 5(b)]. Fig. 5(b) presents some data for a major tidal cycle, during the same field study data shown in Fig. 5(a). Finally the results showed that the probability distribution functions of $\rho v_x v_z$ were not Gaussian.

Turbulence Time Scales

The integral time scale of a velocity component is a measure of the longest connection in the turbulent behavior of that velocity component. Some time variations of longitudinal integral time scales T_{E_x} are shown in Fig. 6(a) for a major tidal cycle during neap and spring tide conditions. In Fig. 6(a), the axes have a logarithmic scale and the units are in milliseconds. The integral

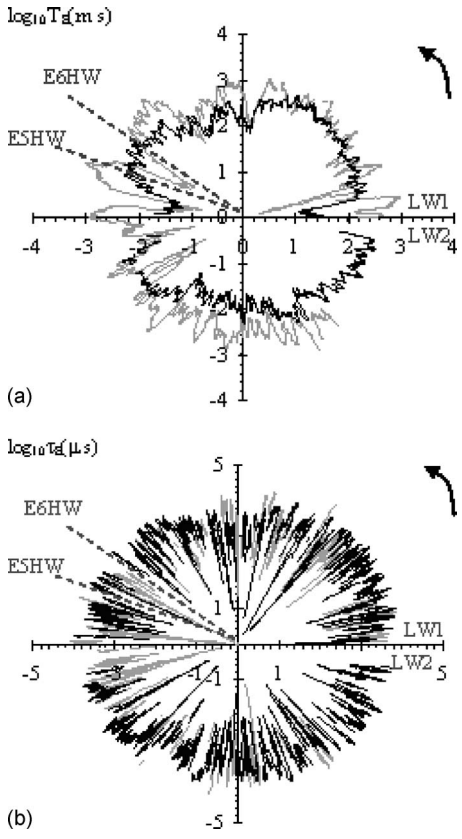

Fig. 6. Longitudinal turbulent time scales during major tidal cycle for neap and spring tide conditions: (●) Field Study E5 (spring tide) ADV with sensor at 0.1 m above bed; and (●) Field Study E6 (neap tide) with ADV sensor at 0.4 m above bed. Axes have a logarithmic scale: (a) integral time scale T_{E_x} (ms); (b) dissipation time scale τ_{E_x} (μs)

time scales of longitudinal velocity T_{E_x} were larger during the flood tide than during the ebb tide [Fig. 6(a)]. For that data set, the horizontal integral time scales were typically between 0.4 and 2 s at 0.2 m above the bed and between 0.06 and 1 s at 0.4 m above the bed.

The dissipation time scale τ_E is a measure of the most rapid changes that occur in the fluctuations of a velocity component and of the smaller eddies that are primary responsible for the dissipation of energy. Fig. 6(b) shows some time variations of longitudinal dissipation time scales τ_{E_x} for a major tidal cycle during neap and spring tide conditions. Note that the axes have a logarithmic scale and the units are in microseconds. The dissipation time scale data seemed independent of the tidal phase [Fig. 6(b)]. They were typically about 0.002–0.02 s for all field studies, independent of the tidal conditions, vertical elevations, and longitudinal sampling location. Such dissipation time scales were consistently smaller than the time between two consecutive samples: e.g., $1/F_{\text{scan}}=0.04$ s for $F_{\text{scan}}=25$ Hz. The findings showed that a high-frequency sampling is required to capture a range of eddy time scales relevant to the dissipation processes, and that the sampling rates must be at least 20–50 Hz.

The analysis of integral and dissipation time scales of all velocity components showed no obvious trend with tidal phase for both neap and spring tide conditions. During the present field studies, the dimensionless transverse and vertical integral time scales were, respectively, $T_{Ey}/T_{Ex}\sim 1$ and $T_{Ez}/T_{Ex}\sim 2-3$. In a tidal channel in southern Australia, Osonphasop (1983) observed $T_{Ey}/T_{Ex}\sim 1.7$ and $T_{Ez}/T_{Ex}\sim 2.2$.

Conclusion

The present field data were collected in a small subtropical estuary corresponding to a small drowned river valley (coastal plain) type with a limited, sporadic freshwater inflow and a cross section that deepens and widens toward the mouth. The results illustrated the significant influence of tidal forcing for this type of small estuary. During spring tides, the turbulent velocity fluctuations and Reynolds stress fluctuations were much larger than during neap tide conditions with a more asymmetrical response. Some turbulent properties were similar to classical turbulent boundary layer results, including the vertical turbulence ratio v_z'/v_x', the skewness and excess kurtosis of the velocity components, and time-averaged tangential stress data. Other results differed from classical boundary layer properties, including the horizontal turbulence intensity v_y'/v_x', while the probability distribution functions the turbulent stresses were not Gaussian. Further multiple flow reversals were observed at high waters, most noticeably during neap tides and in the upper estuary.

Continuous turbulent velocity sampling at relatively high frequency allowed a characterization of the turbulence field and its variations with time. A striking feature of the present data sets was the rapid and large fluctuations in all turbulence characteristics during the tidal cycle. This was rarely documented in previous studies, but an important characteristic of the present study is the continuous high-frequency sampling over relatively long periods. The findings showed that the turbulence properties, and integral time and length scales, should not be assumed constant in a small estuary. The present results show, in particular, a different response of small subtropical estuaries from that observed in larger estuaries.

Acknowledgments

The writers acknowledge the strong support of Dr. Ian Ramsay and John Ferris (Qld E.P.A.).

References

Chanson, H., Brown, R., Ferris, J., Ramsay, I., and Warburton, K. (2005a). "Preliminary measurements of turbulence and environmental parameters in a sub-tropical estuary of eastern Australia." *Environmental Fluid Mechanics*, 5(6), 553–575.

Chanson, H., Trevethan, M., and Aoki, S. (2005b). "Acoustic Doppler velocimetry (ADV) in a small estuarine system. field experience and 'despiking.'" *Proc., 31st Biennial IAHR Congress*, Seoul, Korea, B. H. Jun, S. I. Lee, I. W. Seo, and G. W. Choi, eds., Theme E2, Paper 0161, 3954–3966.

Fransson, J. H. M., Matsubara, M., and Alfredsson, P. H. (2005) "Transition induced by free-stream turbulence." *J. Fluid Mech.*, 527, 1–25.

Hallback, M., Groth, J., and Johansson, A. V. (1989). "A Reynolds stress closure for the dissipation in anisotropic turbulent flows." *Proc., 7th Symp. Turbulent Shear Flows*, Vol. 2, Stanford University, Stanford, Calif., 17.2.1–17.2.6.

Ham, R. van der, Fromtijn, H. L., Kranenburg, C., and Winterwerp, J. C. (2001). "Turbulent exchange of fine sediments in a tidal channel in the Ems/Dollard Estuary. Part I: Turbulence measurements." *Cont. Shelf*

Res., 21, 1605–1628.
Kawanisi, K., and Yokosi, S. (1994). "Mean and turbulence characteristics in a tidal river." *Cont. Shelf Res.*, 17(8), 859–875.
Nezu, I., and Nakagawa, H. (1993). "Turbulence in open-channel flows." *IAHR Monograph*, IAHR Fluid Mechanics Section, Balkema, Rotterdam, The Netherlands.
Niederschultze, M. A. (1989). "Turbulent flow through a rectangular channel." Ph.D. thesis, University of Illinois, Urbana-Champaign, Ill.
Osonphasop, C. (1983). "The measurements of turbulence in tidal currents." Ph.D. thesis, Monash Univ., Melbourne, Australia.
Shiono, K., and West, J. R. (1987). "Turbulent perturbations of velocity in the Conwy Estuary." *Estuarine Coastal Shelf Sci.*, 25, 533–553.
Tachie, M. F. (2001). "Open channel turbulent boundary layers and wall jets on rough surfaces." Ph.D. thesis, Univ. of Saskatchewan, Saskatchewan, Canada.
Trevethan, M., Chanson, H., and Brown, R. J. (2006). "Two series of detailed turbulence measurements in a small subtropical estuarine system." *Rep. No. CH58/06*, Div. of Civil Engineering, The Univ. of Queensland, Brisbane, Australia.
Voulgaris, G., and Meyers, S. T. (2004). "Temporal variability of hydrodynamics, sediment concentration and sediment settling in a tidal creek." *Cont. Shelf Res.*, 24, 1659–1683.
Xie, Q. (1998). "Turbulent flows in non-uniform open channels: Experimental measurements and numerical modelling." Ph.D. thesis, Univ. Of Queensland, Brisbane, Australia.